ACS APPLIED MATERIALS & INTERFACES

Research Article

www.acsami.org

Densely Packed Siloxane Barrier for Blocking Electron Recombination in Dye-Sensitized Solar Cells

Donghoon Song,[†,§] Hyosung An,[‡,§] Jung Hyun Lee,[†] Jung Lee,[‡] Hyungwoo Choi,[†] In Sung Park,[‡] Jong-Man Kim,*[,‡] and Yong Soo Kang*[,†]

[†]Center for Next Generation Dye-Sensitized Solar Cells and Department of Energy Engineering, and [‡]Department of Chemical Engineering, Hanyang University, Seoul 133-791, Korea

Supporting Information

ABSTRACT: A challenge in developing photovoltaic devices is to minimize the loss of electrons, which can seriously deteriorate energy conversion efficiency. In particular, minimizing this negative process in dye-sensitized solar cells (DSCs) is imperative. Herein, we use three different kinds of siloxanes, which are adsorbable to titania surfaces and polymerizable in forming a surface passivation layer, to reduce the electron loss. The siloxanes used are tetraethyl orthosilicate (TEOS or compound A), 1-(3-(1*H*-imidazol-1-yl)propyl)-3-(3-triethoxysilyl) propyl) urea (compound B), and *N*-(3-triethoxysilylpropyl)-*N*′[3-(3-methyl-1*H*-imidazol-3-ium) propyl] urea iodide (compound C). Titania surface passivation by either compound B or C was comparatively more effective in increasing the electron lifetime than TEOS. In the case of small-sized TEOS combined with either large-sized compound B or C, a thinner and denser passivation layer was presumably developed, thus increasing electron lifetime further. Intriguingly, device AB shows the longest electron lifetime, whereas device AC has the highest energy conversion efficiency among these experimental conditions. These results suggest that, in this special case, the electron lifetime may not be a dominant parameter in determining the energy conversion efficiency.

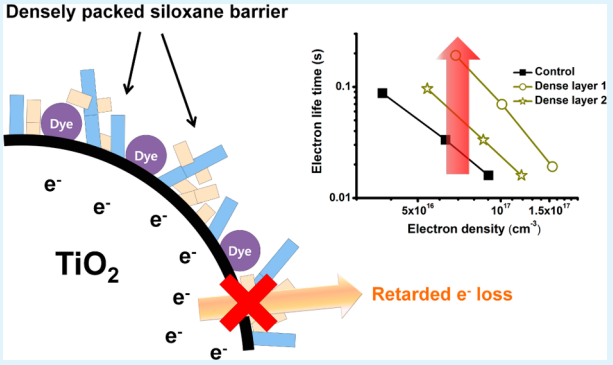

KEYWORDS: *siloxanes, coadsorbents, dense packing, electron recombination, dye-sensitized solar cells*

INTRODUCTION

Dye-sensitized solar cells (DSCs), which are characterized not only by low cost electricity generation, but also by versatile applications such as flexible, aesthetic, or hybrid devices, have drawn great interest in both academia and industry.[1] DSCs adopt a photoanode with a tremendous surface area via a mesoporous semiconductor, typically TiO_2, to provide sufficient sites for dye anchoring, resulting in efficient light harvesting and remarkable energy conversion with over 11% efficiency.[2−4] However, the huge interfacial area of the TiO_2 mesoporous electrode concomitantly increases the unintentional charge recombination sites through the TiO_2/electrolyte interface. Moreover, another electron recombination occurs at the TCO/electrolyte interface where the charges are collected. In certain cases, this electron loss significantly deteriorates the cell performance of solar cells; thus how to passivate the TCO/electrolyte interface is an important research topic.[5−9]

Practically, TiO_2 interfacial recombination processes can be retarded through modification of the TiO_2 surface. One simple and typical way is to use coadsorbing materials together with dye.[10−23] To some extent, the coadsorbent treatment deactivates the empty sites of the TiO_2 surface, through which the electron recombination occurs with oxidized redox species, typically I_3^-. In addition, the conduction band (CB) of the TiO_2 can be displaced, depending on the physicochemical properties of the coadsorbents. In particular, certain link groups, such as carboxylic and phosphoric acids, cause a downward CB shift. The magnitude and direction of the dipole moment of the coadsorbent molecule also affect the CB shift to some extent.[12,13] Thereby, the improvement of total energy conversion efficiency will be achieved by blocking the electron recombination and/or suitably tuning the CB energy level through the proper choice of coadsorbents, through the enhancement of either the photocurrent or the photovoltage, and, in the best cases, both. Several coadsorbents, containing phosphonic acids[13,14] and carboxylic acids,[11,15,16] have been applied to modify the dyed photoanode surface to enhance the performance of DSCs. For instance, surface modification with a phosphonic acid coadsorbent, with the negative ends directed toward the substrate surface, causes a TiO_2 CB level shift, giving rise to a higher V_{oc} as well as J_{sc}.[17] Two zwitterionic butyric acid coadsorbents, 4-guanidinobutyric acid and 4-aminobutyric acid,[13] also result in the improvement of the cell performance. The former passivation device shows a higher V_{oc} due to the upward CB shift, whereas the latter shows a

Received: April 17, 2014
Accepted: July 10, 2014
Published: July 10, 2014

downward CB shift, enhancing J_{sc} with slightly lower open-circuit voltage.

Meanwhile, a few groups have used silanes or siloxanes as coadsorbents.[18−22] In one such case, the recombination rates decreased by passivating the TiO_2 surface with tricholoromethylsilane, a highly reactive silane reagent, utilizing the vapor-phase silanization procedure in the iodide-free redox couple.[18,19] They found that the formation of poly(methyl siloxane) on the TiO_2 surface effectively decreases the back electron transfer toward the oxidized redox couple and, therefore, improves the performance of the DSCs. Use of triethoxysilane in ethanol solution has also been reported to optimize the treatment.[22]

In this study, we aimed to form a dense and compact passivation layer by modifying the N719 dye-anchored TiO_2 surface with two different and large-sized siloxanes (Figure 1),

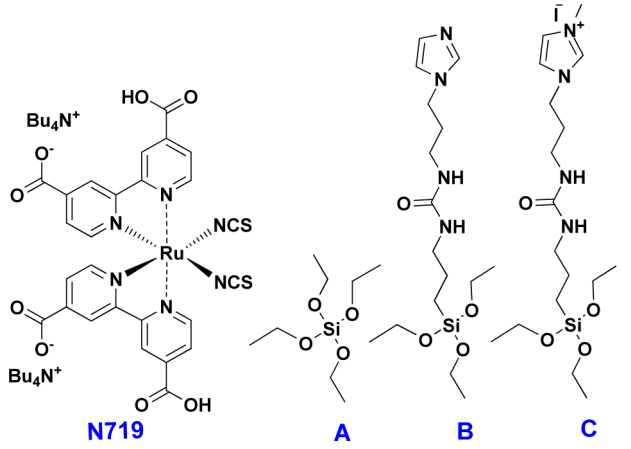

Figure 1. Chemical structures of a N719 dye and the three siloxanes, TEOS (compound A, molecular length: 9.3 Å), compound B (18.9 Å), and compound C (19.4 Å).

combined with a small-sized siloxane in ethanol solution, via their surface anchoring reactions to the TiO_2 surface and subsequent condensation or polymerization reactions (Scheme 1). The siloxanes used are 1-(3-(1*H*-imidazol-1-yl)propyl)-3-(3-triethoxysilyl) propyl) urea (compound B) and *N*-(3-triethoxysilylpropyl)-*N*′[3-(3-methyl-1*H*-imidazol-3-ium) propyl] urea iodide (compound C), as well as tetraethyl orthosilicate (TEOS or compound A).[24] It was found that the passivation by compound B or C was fairly successful in slowing the recombination reaction. Furthermore, when small-sized TEOS (or A) was combined with either large-sized compound B or C, the electron lifetime was further increased, presumably due to the formation of the more densely packed poly(siloxane) layer. Interestingly, however, the reduced electron recombination rate did not ensure the improvement of the energy conversion efficiency in the case of DSCs, as evidenced in devices B and AB.

Scheme 1. Schematic Diagram of Hydrolysis and Passivation Mechanism of Siloxanes: (a) Hydrolysis, (b) Surface Anchoring Reaction, and (c) Condensation/Polymerization

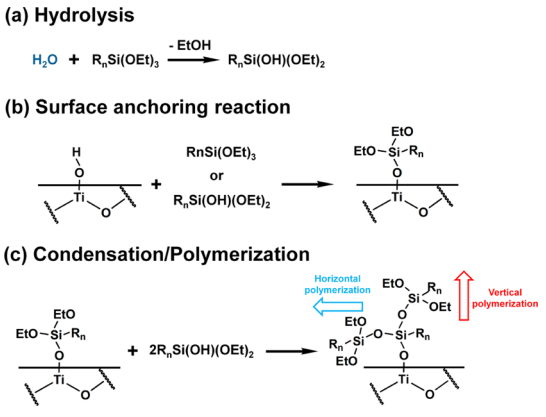

EXPERIMENTAL SECTION

1. Materials and Reagents. All reagents were used as received. Sensitizing ruthenium dye N719 ($RuL_2(NCS)_2$:2TBA (L = 2,2′-bipyridyl-4,4′-dicarboxylic acid; TBA = tetrabutylammonium)) was obtained from Solaronix (Switzerland). TEOS was purchased from Aldrich. Compounds B and C were prepared according to the previously published methods.[24] The electrolyte consists of 0.6 M 1-methyl 3-propyl imidazolium iodide (MPII), 0.03 M I_2, and 0.5 M 4-*tert*-butylpyridine (tBP) in the mixture solvent of acetonitrile (AN) and valeronitrile (VN) (1:1, v/v).

2. Device Fabrication. FTO glasses were cleaned sequentially in isopropyl alcohol, deionized water, and ethanol, using an ultrasonic bath for 15 min. Any solvent residue was removed in a vacuum oven for 30 min. A TiO_2 blocking layer was prepared by $TiCl_4$ treatment, followed by annealing in the air at 450 °C for 30 min. A 5.5-μm thick transparent TiO_2 mesoscopic film was coated onto the FTO glass, TEC-8 (~8 Ω/cm^2, Pilkington), and a 4-μm thick scattering layer was deposited onto the transparent TiO_2 layer by the doctor-blade technique with commercial TiO_2 pastes (Dyesol 18 NR-T and Dyesol WER 2-O, respectively) resulting in a square-shaped active area of 0.26 cm^2. After the layer-by-layer deposited TiO_2 film was annealed at 450 °C for 30 min, the $TiCl_4$ treatment was repeated as previously described. After being cooled to 80 °C, the prepared TiO_2 electrodes were immersed into a 0.3 mM N719 solution in AN:*tert*-butanol (1:1 v/v) at 30 °C for 24 h. The films were then rinsed to remove excess dye, and then stored in a vacuum oven for 30 min to remove any solvent. To passivate the dyed TiO_2 surfaces, each photoanode was immersed in five coadsorbent solutions in anhydrous ethanol (0.3 M TEOS (A), 0.3 M B, 0.3 M C, 0.3 M equimolar mixture of TEOS (A) and B, and 0.3 M equimolar mixture of TEOS (A) and C) at 30 °C for 4 days, and rinsed with anhydrous ethanol. The counter electrodes were thermally platinized at 450 °C for 30 min, using H_2PtCl_6 solution. The TiO_2 substrate and Pt counter electrode were assembled using a Surlyn frame, Meltonix 1170-25 (Solaronix). The electrolyte was injected through the hole in the counter substrates, and, finally, the DSCs were sealed with sealants under a thin glass cover by heating to produce the control cell, device A, device B, device AB, device C, and device AC (with and without TEOS (A), B, C, TEOS (A)/B, and TEOS (A)/C, respectively).

3. Photovoltaic Characterization. For the *J*−*V* characteristics, a 300 W xenon light source (Newport, U.S.) was used to give an irradiance of 1 sun illumination at AM 1.5 (100 mW cm^{-2}) at the surface of the solar cell. The light intensity was calibrated by a silicon solar cell (PV Measurements, Inc.). The data were recorded by application of an external potential bias to the cell and measuring the generated photocurrent with a Keithley model 2400 digital source meter (Keithley, U.S.). A shading mask with an aperture of 0.36 cm^2 was applied to each cell, preventing the overestimation of energy conversion efficiency.

4. Spectroscopic Measurements. The attenuated total reflection Fourier transform infrared (ATR-FTIR) spectra were measured using a JASCO FT/IR-4200 spectrometer with an ATR PRO450-S accessory and a ZnSe crystal. The spectra for the stained TiO_2 surfaces were scanned from 4000 to 400 cm^{-1} at a resolution of 4 cm^{-1} with 64 scans; no ATR correction was applied to the data. UV−visible spectra of dye-sensitized TiO_2 electrodes were recorded on a single beam Agilent 8453 UV−visible spectrometer. The X-ray

photoelectron spectroscopy (XPS) was collected using a VG Microtech (VG Multilab ESCA 2000 system) X-ray photoelectron spectrometer. The XPS experiment was carried out in a high-vacuum chamber under a base pressure of 3×10^{-9} Torr, and the samples were excited with Al Kα X-ray radiation of 1487 eV energy. All of the spectra reported in this work are referenced and calibrated to Ti 2p peak (458.6 eV).[25]

5. Photoelectrochemical Measurements. After calibration by a silicon reference cell, the incident photon-to-current conversion efficiency (IPCE) spectra of DSCs were measured as a function of wavelength in the range of 300−800 nm with a chopping wavelength of 10 nm using a model QEX7 solar cell spectral response measurement system (PV Measurements, Inc.). The beam size was slightly larger than cell active area, thus requiring repeated measurement. The intensity-modulated photovoltage spectroscopy (IMVS) using the CIMPS (Controlled Intensity Modulated Photo Spectroscopy) system (Zahner) was employed to give insight into the charge recombination at the TiO_2/electrolyte interface.[26] IMVS provides information on electron lifetime (τ_n) under open-circuit conditions. Intensity-modulated photocurrent spectroscopy (IMPS) using the CIMPS system employs the same light perturbation as IMVS, but measures the kinetics of charge collection under short-circuit conditions.[27] Charge extraction methods using CIMPS (Zahner) have been employed to measure the electron density as a function of V_{oc}.[28] Devices were illuminated with a red light source for 5 s and held at open-circuit conditions. The light source was switched off, and the charge was extracted simultaneously while changing the DSCs condition to a short circuit given milliseconds or seconds voltage-decay time. The electron density was calculated from the amount of extracted charge and the volume of the TiO_2 film without considering the porosity of the electrode.

RESULTS AND DISCUSSION

The siloxanes were first anchored on the OH-group-containing TiO_2 surface, and subsequently condensation-polymerized to form a thin layer as illustrated in Scheme 1.[29,30] During the passivation process, the siloxane layer was formed by vertical and horizontal polymerization as shown in Scheme 1. Vertical polymerization may build up a thick layer, whereas horizontal polymerization may induce a dense layer. However, siloxanes like compound B or C may develop a loosely packed geometry due to their bulky chains, which can allow the electron acceptor I_3^- in the electrolyte to approach the electrons in TiO_2 without difficulty, deteriorating surface passivation effects. In an attempt to increase the molecular packing density, we introduced small-sized siloxane TEOS (compound A) into either the large-sized compound B or C (Scheme 2). It is reasonable to remark that compound B or C can produce a dense network when combined with TEOS; TEOS may link randomly anchored compound Bs or Cs together. In addition, TEOS may also self-polymerize, increasing the density of the layer.

The attenuated total reflection Fourier transform infrared (ATR-FTIR) spectra of the mesoporous TiO_2 anchored with the siloxanes are illustrated in Figure 2. The peak at 930 cm^{-1} arises from the Si−O−Ti bond, whereas the broad peak at around 1070 cm^{-1} is caused by the Si−O−Si stretching vibration.[30,31] These peaks imply that the siloxanes are successfully anchored at the TiO_2 surface to form Ti−O−Si bonds and are polymerized vertically or horizontally to form Si−O−Si bonds. Upon comparing the intensity of the Si−O−Si peak, it appears that the polymerization of compound C is much faster than the others because of the large amount of water inherently present near hydrophilic compound C; polymerization of the siloxanes is facilitated by the silanization-catalyst H_2O.[32] We therefore expect that the treated layer

Scheme 2. Schematic Diagram of (a) Loose Packing via Compound B or C Only and (b) Dense Packing via Compound B or C Combined with A, TEOS

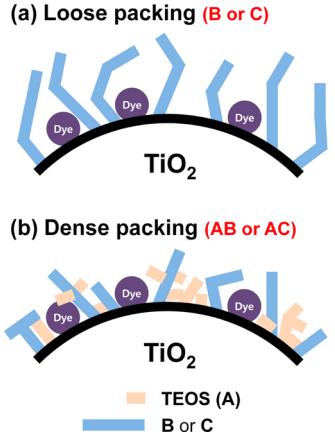

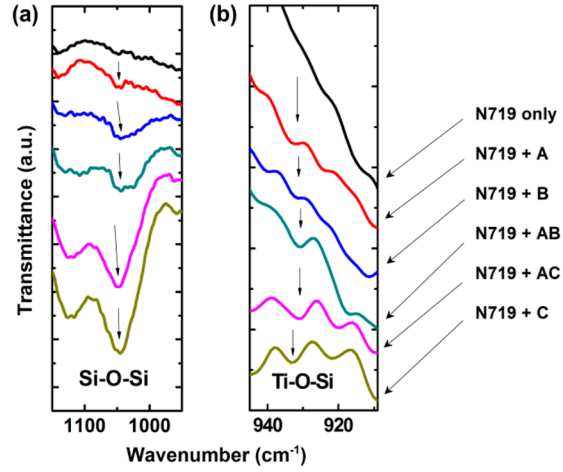

Figure 2. ATR-FTIR spectra of TiO_2 films immobilized with N719 sensitizing dye alone, N719/three siloxanes, and N719/two equimolar mixtures of siloxanes, B/TEOS and C/TEOS, for (a) Si−O−Si and (b) Ti−O−Si bonds.

thickness will increase in the order of TEOS < compound B < compound C.

Specifically, we evaluated the mean thickness of the siloxane-treated layer relative to TiO_2 from the X-ray photoelectron spectroscopy (XPS) data as shown in Figure 3. Note that the degree of damping of the Ti 2p intensity in the XPS relative to

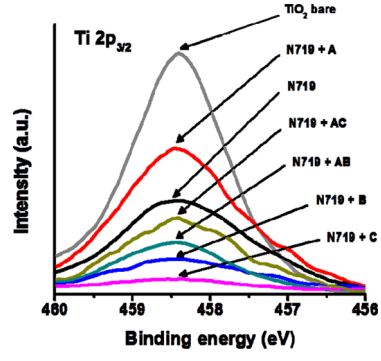

Figure 3. Ti $2p_{3/2}$ peaks in the XPS data of N719-sensitized TiO_2 films with or without treatment by siloxanes, A, B, C, A+B, and A+C.

Table 1. $J-V$ Characteristics[a] for Devices under 1 sun Irradiation, and the Relative Amount[b] of Dyes Loaded on the TiO_2 Film

	dye and coadsorbent	J_{SC} (mA/cm^2)	V_{OC} (mV)	FF	η (%)	relative dye loaded	J_{SC}/(relative dye loaded) (mA/cm^2)
control	N719 only	9.5 ± 0.0	797 ± 4	73.9 ± 0.1	5.6 ± 0.0	1.00	9.5 ± 0.0
device A	N719 + TEOS	9.7 ± 0.1	785 ± 3	72.9 ± 0.8	5.6 ± 0.0	0.68	14.3 ± 0.1
device B	N719 + B	8.3 ± 0.1	824 ± 0	70.7 ± 0.3	4.8 ± 0.1	0.76	10.9 ± 0.1
device AB	N719 + TEOS + B	8.2 ± 0.1	828 ± 1	69.5 ± 0.3	4.7 ± 0.0	0.76	10.8 ± 0.1
device C	N719 + C	10.2 ± 0.4	778 ± 10	73.7 ± 0.0	5.9 ± 0.2	0.77	13.2 ± 0.5
device AC	N719 + TEOS + C	10.8 ± 0.1	777 ± 6	73.6 ± 0.7	6.2 ± 0.1	0.57	18.9 ± 0.2

[a]Values obtained represent the average over four devices for each experiment. The cell-active areas were 0.27 cm^{-2}. [b]This is estimated by the detachment of the remaining dyes on the TiO_2 surface with 10 mM KOH solution for an hour after the coadsorbing process.

the pristine TiO_2 surface can suggest the mean thickness of the passivation layer onto the TiO_2 surface.[19,33] The relationship is described in eq 1:

$$I(d) \propto I_0 \cdot e^{-d/\lambda} \quad (1)$$

where $I(d)$ is the substrate intensity for a layer of thickness d, I_0 represents the intensity of the pristine TiO_2 surface, and λ represents the mean free path depending on the electron energy. Here, the λ of photoelectrons of all samples was assumed to be 18 Å.[33] Thus, a lower Ti 2p intensity implies a thicker layer. The thickness, d, of the passivation layer was then quantitatively estimated: the substrates with N719, N719 + A, N719 + B, N719 + C, N719 + AB, and N719 + AC have a mean thicknesses of 1.8, 0.9, 3.8, 6.2, 3.0, and 2.2 nm, respectively. Note that the pristine N719 layer, in this case, is thicker relative to the reported thickness of ∼1 nm.[34] In particular, the mean thickness of the N719 + A layer is reduced by one-half, relative to that of the N719 layer, implying that some N719 dyes are removed by the TEOS treatment. This is consistent with the amount of dyes adsorbed on the surface, as listed in Table 1. The reduced thicknesses of the substrates containing AB or AC, observed relative to those with only B or only C, respectively, suggest the formation of compact layers. Meanwhile, the relative ratios of Ru to Si were measured and summarized in Supporting Information Figure S3 and Table S1. The Si amount follows N719 + A < N719 + AB < N719 + B < N719 + AC < N719 + C at a constant Ru amount. Also, it roughly corresponds to the thickness of the siloxanes, suggesting that the compact layers do not carry excess amount of Si at a same thickness. As discussed in detail in the following section, these compact layers eventually decreased the electron recombination, indicating the formation of densely packed layers by siloxanes, AB, or AC.

The electron lifetime, τ_e, as a measure of electron recombination (Figure 4), partly corresponds to the ATR-FTIR and XPS evidence suggested previously. The τ_e of the devices was obtained with the support of intensity-modulated photovoltage spectroscopy (IMVS)[26] and charge extraction (CE)[28] methods. The outcomes after the siloxanization are quite dramatic, except for device A with TEOS. The data suggest, in view of the passivation effects on the recombination reaction, that the treatment by compound B is the most effective, and that compound C is also quite successful. Furthermore, incorporating small-sized TEOS molecules with these two asymmetric siloxanes caused an additional decrease in the recombination as a result of dense packing. The order of electron lifetimes is listed in increasing order: device A < control < device C < device AC < device B < device AB. As was previously shown in Figures 2 and 3, and Supporting Information Table S1, the TEOS layer seems a little too thin to efficiently block the recombination as much as the N719

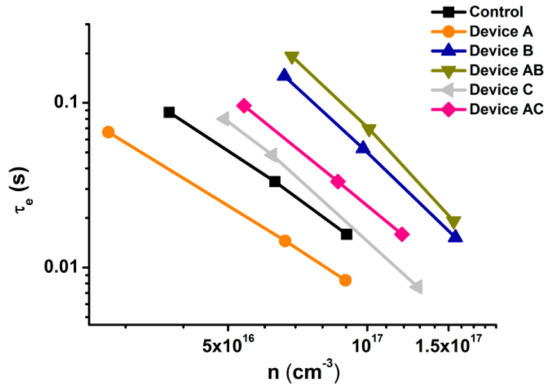

Figure 4. Electron lifetime versus electron density of the control and devices treated by compounds A, B, C, AB, and AC derived from measurements of CE and IMVS.

layer in addition to detachment of dye molecules. The reason compound B was the most effective in reducing the recombination may be partly attributable to the complexation of nitrogen lone-pair electrons in imidazole with free iodine, the electron recombination species.[35]

Photovoltaic performances of the DSCs were evaluated under 1 sun illumination conditions (AM 1.5G, 100 mW/cm^2), as seen in Figure 5. Short-circuit current density (J_{SC}), open-

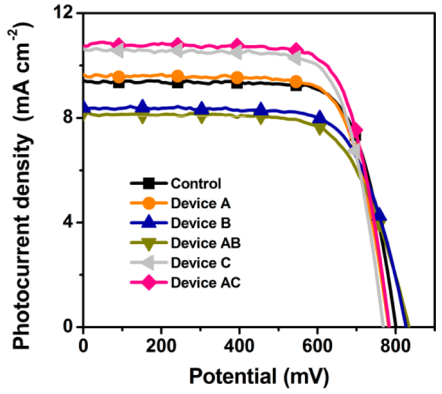

Figure 5. Representative $J-V$ curves for all devices measured under 1 sun conditions.

circuit voltage (V_{OC}), fill factor (FF), and photovoltaic conversion efficiency (η) are listed in Table 1. Devices containing compound C yielded higher J_{SC} values, whereas devices containing compound B yielded higher V_{OC} values. Interestingly, device A, with TEOS only, did not contribute to the enhancement of η, as compared to the control. It is notable that device AC, which employed the equimolar mixture of compounds A and C, showed enhanced η by 11% (5.6% →

6.2%), arising from the increase in the J_{SC} by 14% (9.5 → 10.8 mA/cm^2). However, device AB, using the equimolar mixture of compounds A and B, showed a reduction in η of 16% (5.6% → 4.7%) due to the decrease in the J_{SC} by 14% (9.5 → 8.2 mA/cm^{-2}).

To understand these findings, we utilized photoelectrochemical analyses. To elucidate the tendency of J_{SC} values with respect to wavelength, we recorded the IPCE spectra (Figure 6)

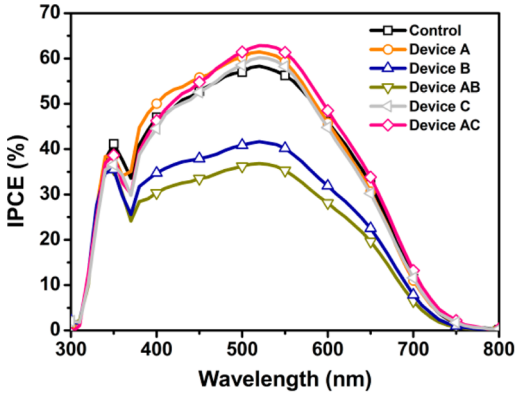

Figure 6. External quantum efficiency spectra of each representative device with wavelength of incident light.

by tracing quantum efficiency at light wavelengths of 300−800 nm. As seen in Figure S4 (Supporting Information), it might be anticipated that the light absorption by compound B or C would have a slight effect on IPCE around 400 to 450 nm. Devices C and AC, displaying larger J_{SC} values than the control, show entirely higher quantum yield regardless of the light wavelength. $\eta_{IPCE}(\lambda)$ is expressed as

$$\eta_{IPCE}(\lambda) = \eta_{LH}(\lambda)\eta_{INJ}(\lambda)\eta_{COL}(\lambda) \quad (2)$$

where $\eta_{LH}(\lambda)$ is light harvesting, $\eta_{INJ}(\lambda)$ is electron injection, and $\eta_{COL}(\lambda)$ represents charge collection efficiencies. Hence, we investigated three parameters, $\eta_{LH}(\lambda)$, $\eta_{INJ}(\lambda)$, and $\eta_{COL}(\lambda)$, to understand the difference in IPCE spectra in the measured region of 300−800 nm. First, η_{LH} of the devices is easily understood in terms of the amount of loaded dye. During the siloxane treatment, a large amount of dye (24−43%) was detached, as shown in Table 1, indicating the η_{LH} is definitely lowered.

The CE technique was used to obtain information on the trap states in TiO_2 and, consequently, on the CB position in TiO_2.[28] It is worth noting that the CB position may be changed by molecules adsorbed to the TiO_2 surface such as dyes, electrolyte species, and coadsorbents.[1,13,17,36,37] In Figure 7, the electron density (n), estimated from the CE data, is depicted as a function of open-circuit voltage (V_{OC}), revealing an important insight into the CB shift of the devices. In the case of devices C and AC, there is a noticeable downward CB movement by approximately 50 mV, presumably attributable to the positively charged imidazolium cation of compound C. Many preceding reports emphasize the fact that the downward shift of the CB guarantees an increased η_{INJ} to provide more driving force for electron injection.[1,13,38] Therefore, it is plausible to conclude that devices containing C molecules retain a higher η_{INJ} as a result of the downward shift of the CB, that is, the increase in the density of accepting states in TiO_2 CB.[38]

All devices, excluding devices B and AB, showed enhanced J_{SC} values as compared to the control, even though the amount

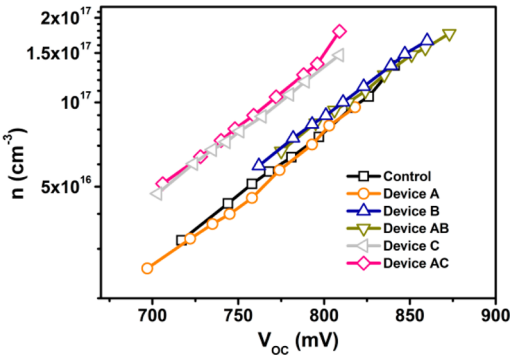

Figure 7. TiO_2 electron density versus open-circuit voltage of the devices evaluated by the charge extraction method.

of N719 was greatly decreased (43%) in the case of device AC. It is believed that the relaxation of the dye aggregate by siloxanes might increase the efficiency of dyes to some extent, which could result in the increment of η_{INJ}.[39,40] This could be supported by the comparison of photocurrent at fixed dye load where all devices showed higher photocurrent relative to the control cell (Table 1). This aspect is clear because device A showed a marginally increased J_{SC} value as compared to the control device, despite the fact that the TEOS treatment led to a decrease in the dye load up to 32%, with faster recombination and similar electron-injection driving force as shown in Figures 4 and 7, respectively. Meanwhile, the UV−vis absorption spectra for six photoelectrodes were obtained and depicted in Figure 8. The blue-shifted peaks for the electrodes coadsorbed

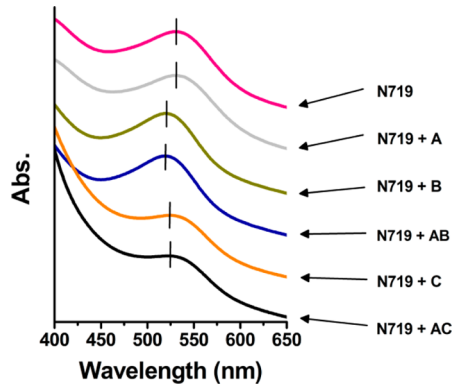

Figure 8. UV−visible absorption spectra of N719-sensitized TiO_2 films with or without treatment by siloxanes.

with compounds B and AB appear at around 520 nm, deviated by ∼10 nm as compared to the others; this presumably represents the larger extent of dye aggregates and/or the dye/compound B complex. The dye/compound B complex may have formed because the lone-pair electron of the imidazole nitrogen of compound B interacts with the carboxylic acids of N719, leading to the η_{INJ} decreasing.[39−43] We believe this could be a main reason for the low J_{SC} values for devices B and AB.

Meanwhile, the η_{COL} could be interpreted in terms of the electron diffusion and the electron lifetime through the TiO_2 layer. The electron diffusion coefficient was estimated using the data from IMPS (Figure S5, Supporting Information), and showed very similar values, regardless of the devices. The electron lifetime, τ_e, was also evaluated and previously illustrated in Figure 4.[44] Considering the negligible difference in the electron diffusion coefficients among all of the devices,

the electron lifetime can be correlated directly with the η_{COL}. However, the η_{COL} does not seem to significantly affect the J_{SC}.

V_{OC} containing compounds B and AB increased relative to that of the control, whereas those containing compounds C and AC slightly decreased (Table 1). V_{OC} is significantly affected by the electron recombination reaction. Although the recombination is slowed, DSCs with compound C or AC do not retain higher V_{OC} values as compared to the control. This is because the TiO_2 CB energy level, as well as the electron recombination, contribute to the V_{OC}.[1] A 50 mV downward shift of the CB was observed for compound C and AC (Figure 7); this led to V_{OC} values of these devices that were lower than that of the control.

CONCLUSIONS

Three siloxanes, TEOS (A) and compounds B and C, are coadsorbed onto the N719-sensitized TiO_2 film by a simple and cost-effective liquid-state process. Both compounds B and C are more effective than TEOS in increasing both the electron lifetime, which represents the retarded electron recombination, and the energy conversion efficiency. When small-sized TEOS is combined with either large-sized compound B or C, the electron lifetime is further increased, presumably due to the formation of a more densely packed siloxane layer. Intriguingly, we found that device AB shows the longest electron lifetime, whereas device AC had the highest energy conversion efficiency. The high efficiency for device AC may be mostly due to the increased photocurrent originating from the enhanced efficiencies of both electron injection and collection at the expense of the small downward CB shift.

ASSOCIATED CONTENT

Supporting Information

TGA-DSC, UV−vis absorption, and full-range ATR-FTIR results, electron diffusion coefficient by IMPS, and photovoltaic performance transient data. This material is available free of charge via the Internet at http://pubs.acs.org.

AUTHOR INFORMATION

Corresponding Authors

*E-mail: jmk@hanyang.ac.kr.
*E-mail: kangys@hanyang.ac.kr.

Author Contributions

[§]These authors contributed equally.

Notes

The authors declare no competing financial interest.

ACKNOWLEDGMENTS

This work was supported by the National Research Foundation of Korea (NRF) grant funded by the Korean government (MSIP) for the Center for Next Generation Dye-sensitized Solar Cells (no. 2013004800) and by the Korea Center for Artificial Photosynthesis (KCAP) (no. 2009-0093883).

REFERENCES

(1) Hagfeldt, A.; Boschloo, G.; Sun, L.; Kloo, L.; Pettersson, H. Dye-Sensitized Solar Cells. *Chem. Rev.* **2010**, *110*, 6595−6663.

(2) Yella, A.; Lee, H.-W.; Tsao, H. N.; Yi, C.; Chandiran, A. K.; Nazeeruddin, M. K.; Diau, E. W.-G.; Yeh, C.-Y.; Zakeeruddin, S. M.; Grätzel, M. Porphyrin-Sensitized Solar Cells with Cobalt (II/III)−Based Redox Electrolyte Exceed 12% Efficiency. *Science* **2011**, *334*, 629−634.

(3) Han, L.; Islam, A.; Chen, H.; Malapaka, C.; Chiranjeevi, B.; Zhang, S.; Yang, X.; Yanagida, M. High-Efficiency Dye-Sensitized Solar Cell with A Novel Co-Adsorbent. *Energy Environ. Sci.* **2012**, *5*, 6057−6060.

(4) Cao, Y.; Bai, Y.; Yu, Q.; Cheng, Y.; Liu, S.; Shi, D.; Gao, F.; Wang, P. Dye-Sensitized Solar Cells with a High Absorptivity Ruthenium Sensitizer Featuring a 2-(Hexylthio)thiophene Conjugated Bipyridine. *J. Phys. Chem. C* **2009**, *113*, 6290−6297.

(5) Cameron, P. J.; Peter, L. M. Characterization of Titanium Dioxide Blocking Layers in Dye-Sensitized Nanocrystalline Solar Cells. *J. Phys. Chem. B* **2003**, *107*, 14394−14400.

(6) Xia, J.; Masaki, N.; Jiang, K.; Yanagida, S. Sputtered Nb_2O_5 as a Novel Blocking Layer at Conducting Glass/TiO_2 Interfaces in Dye-Sensitized Ionic Liquid Solar Cells. *J. Phys. Chem. C* **2007**, *111*, 8092−8097.

(7) Lellig, P.; Niedermeier, M. A.; Rawolle, M.; Meister, M.; Laquai, F.; Müller-Buschbaum, P.; Gutmann, J. S. Comparative Study of Conventional and Hybrid Blocking Layers for Solid-State Dye-Sensitized Solar Cells. *Phys. Chem. Chem. Phys.* **2012**, *14*, 1607−1613.

(8) Yella, A.; Heiniger, L.-P.; Gao, P.; Nazeeruddin, M. K.; Grätzel, M. Nanocrystalline Rutile Electron Extraction Layer Enables Low-Temperature Solution Processed Perovskite Photovoltaics with 13.7% Efficiency. *Nano Lett.* **2014**, *14*, 2591−2596.

(9) Góes, M. S.; Joanni, E.; Muniz, E. C.; Savu, R.; Habeck, T. R.; Bueno, P. R.; Fabregat-Santiago, F. Impedance Spectroscopy Analysis of the Effect of TiO_2 Blocking Layers on the Efficiency of Dye Sensitized Solar Cells. *J. Phys. Chem. C* **2012**, *116*, 12415−12421.

(10) Yum, J.-H.; Jang, S.-r.; Humphry-Baker, R.; Grätzel, M.; Cid, J.-J.; Torres, T.; Nazeeruddin, M. K. Effect of Coadsorbent on the Photovoltaic Performance of Zinc Pthalocyanine-Sensitized Solar Cells. *Langmuir* **2008**, *24*, 5636−5640.

(11) Zhang, Z.; Evans, N.; Zakeeruddin, S. M.; Humphry-Baker, R.; Grätzel, M. Effects of ω-Guanidinoalkyl Acids as Coadsorbents in Dye-Sensitized Solar Cells. *J. Phys. Chem. C* **2006**, *111*, 398−403.

(12) Krüger, J.; Bach, U.; Grätzel, M. Modification of TiO_2 Heterojunctions with Benzoic Acid Derivatives in Hybrid Molecular Solid-State Devices. *Adv. Mater.* **2000**, *12*, 447−451.

(13) Wang, M.; Grätzel, C.; Moon, S.-J.; Humphry-Baker, R.; Rossier-Iten, N.; Zakeeruddin, S. M.; Grätzel, M. Surface Design in Solid-State Dye Sensitized Solar Cells: Effects of Zwitterionic Co-adsorbents on Photovoltaic Performance. *Adv. Funct. Mater.* **2009**, *19*, 2163−2172.

(14) Wang, M.; Li, X.; Lin, H.; Pechy, P.; Zakeeruddin, S. M.; Gratzel, M. Passivation of Nanocrystalline TiO_2 Junctions by Surface Adsorbed Phosphinate Amphiphiles Enhances the Photovoltaic Performance of Dye Sensitized Solar Cells. *Dalton Trans.* **2009**, 10015−10020.

(15) Zhang, Z.; Zakeeruddin, S. M.; O'Regan, B. C.; Humphry-Baker, R.; Grätzel, M. Influence of 4-Guanidinobutyric Acid as Coadsorbent in Reducing Recombination in Dye-Sensitized Solar Cells. *J. Phys. Chem. B* **2005**, *109*, 21818−21824.

(16) Li, X.; Lin, H.; Zakeeruddin, S. M.; Grätzel, M.; Li, J. Interface Modification of Dye-Sensitized Solar Cells with Pivalic Acid to Enhance the Open-Circuit Voltage. *Chem. Lett.* **2009**, *38*, 322−323.

(17) Cho, C.-P.; Chu, C.-C.; Chen, W.-T.; Huang, T.-C.; Tao, Y.-T. Molecular Modification on Dye-Sensitized Solar Cells by Phosphonate Self-Assembled Monolayers. *J. Mater. Chem.* **2012**, *22*, 2915−2921.

(18) Gregg, B. A.; Pichot, F.; Ferrere, S.; Fields, C. L. Interfacial Recombination Processes in Dye-Sensitized Solar Cells and Methods To Passivate the Interfaces. *J. Phys. Chem. B* **2001**, *105*, 1422−1429.

(19) Feldt, S. M.; Cappel, U. B.; Johansson, E. M. J.; Boschloo, G.; Hagfeldt, A. Characterization of Surface Passivation by Poly(methylsiloxane) for Dye-Sensitized Solar Cells Employing the Ferrocene Redox Couple. *J. Phys. Chem. C* **2010**, *114*, 10551−10558.

(20) Morris, A. J.; Meyer, G. J. TiO_2 Surface Functionalization to Control the Density of States. *J. Phys. Chem. C* **2008**, *112*, 18224−18231.

(21) Zhang, J.; Yang, G.; Sun, Q.; Zheng, J.; Wang, P.; Zhu, Y.; Zhao, X. The Improved Performance of Dye Sensitized Solar Cells by

Bifunctional Aminosilane Modified Dye Sensitized Photoanode. *J. Renewable Sustainable Energy* **2010**, *2*, 013104.
(22) Son, H.-J.; Wang, X.; Prasittichai, C.; Jeong, N. C.; Aaltonen, T.; Gordon, R. G.; Hupp, J. T. Glass-Encapsulated Light Harvesters: More Efficient Dye-Sensitized Solar Cells by Deposition of Self-Aligned, Conformal, and Self-Limited Silica Layers. *J. Am. Chem. Soc.* **2012**, *134*, 9537−9540.
(23) An, H.; Song, D.; Lee, J.; Kang, E.-M.; Jaworski, J.; Kim, J.-M.; Kang, Y. S. Promotion of Strongly Anchored Dyes on the Surface of Titania by Tetraethyl Orthosilicate Treatment for Enhanced Solar Cell Performance. *J. Mater. Chem. A* **2014**, *2*, 2250−2255.
(24) Tsotsalas, M. M.; Kopka, K.; Luppi, G.; Wagner, S.; Law, M. P.; Schäfers, M.; De Cola, L. Encapsulating ^{111}In in Nanocontainers for Scintigraphic Imaging: Synthesis, Characterization, and In Vivo Biodistribution. *ACS Nano* **2009**, *4*, 342−348.
(25) Johansson, E. M. J.; Hedlund, M.; Siegbahn, H.; Rensmo, H. Electronic and Molecular Surface Structure of Ru(tcterpy)$(NCS)_3$ and Ru(dcbpy)$_2(NCS)_2$ Adsorbed from Solution onto Nanostructured TiO_2: A Photoelectron Spectroscopy Study. *J. Phys. Chem. B* **2005**, *109*, 22256−22263.
(26) Schlichthörl, G.; Huang, S. Y.; Sprague, J.; Frank, A. J. Band Edge Movement and Recombination Kinetics in Dye-Sensitized Nanocrystalline TiO_2 Solar Cells: A Study by Intensity Modulated Photovoltage Spectroscopy. *J. Phys. Chem. B* **1997**, *101*, 8141−8155.
(27) Franco, G.; Gehring, J.; Peter, L. M.; Ponomarev, E. A.; Uhlendorf, I. Frequency-Resolved Optical Detection of Photoinjected Electrons in Dye-Sensitized Nanocrystalline Photovoltaic Cells. *J. Phys. Chem. B* **1999**, *103*, 692−698.
(28) Duffy, N. W.; Peter, L. M.; Rajapakse, R. M. G.; Wijayantha, K. G. U. A Novel Charge Extraction Method for the Study of Electron Transport and Interfacial Transfer in Dye Sensitised Nanocrystalline Solar Cells. *Electrochem. Commun.* **2000**, *2*, 658−662.
(29) Buckley, A. M.; Greenblatt, M. The Sol-Gel Preparation of Silica Gels. *J. Chem. Educ.* **1994**, *71*, 599.
(30) Reddy, J. S.; Sivasanker, S. Selective Oxidation of Cyclohexane over TS-2, A Titanium Silicate Molecular Sieve. *Catal. Lett.* **1991**, *11*, 241−244.
(31) Smith, A. L. *Analysis of Silicones*; Wiley-Interscience: New York, 1974.
(32) Rösch, L.; John, P.; Reitmeier, R. *Silicon Compounds, Organic*; Wiley-VCH Verlag GmbH & Co. KGaA: Weinheim, 2012.
(33) Marinado, T.; Hahlin, M.; Jiang, X.; Quintana, M.; Johansson, E. M. J.; Gabrielsson, E.; Plogmaker, S.; Hagberg, D. P.; Boschloo, G.; Zakeeruddin, S. M.; Grätzel, M.; Siegbahn, H.; Sun, L.; Hagfeldt, A.; Rensmo, H. Surface Molecular Quantification and Photoelectrochemical Characterization of Mixed Organic Dye and Coadsorbent Layers on TiO_2 for Dye-Sensitized Solar Cells. *J. Phys. Chem. C* **2010**, *114*, 11903−11910.
(34) Ellis-Gibbings, L.; Johansson, V.; Walsh, R. B.; Kloo, L.; Quinton, J. S.; Andersson, G. G. Formation of N719 Dye Multilayers on Dye Sensitized Solar Cell Photoelectrode Surfaces Investigated by Direct Determination of Element Concentration Depth Profiles. *Langmuir* **2012**, *28*, 9431−9439.
(35) Kusama, H.; Arakawa, H.; Sugihara, H. Density Functional Study of Imidazole−Iodine Interaction and its Implication in Dye-Sensitized Solar Cell. *J. Photochem. Photobiol., A* **2005**, *171*, 197−204.
(36) Robertson, N. Optimizing Dyes for Dye-Sensitized Solar Cells. *Angew. Chem., Int. Ed.* **2006**, *45*, 2338−2345.
(37) Watson, D. F.; Meyer, G. J. Cation Effects in Nanocrystalline Solar Cells. *Coord. Chem. Rev.* **2004**, *248*, 1391−1406.
(38) Koops, S. E.; O'Regan, B. C.; Barnes, P. R. F.; Durrant, J. R. Parameters Influencing the Efficiency of Electron Injection in Dye-Sensitized Solar Cells. *J. Am. Chem. Soc.* **2009**, *131*, 4808−4818.
(39) Liu, B.; Liu, Q.; You, D.; Li, X.; Naruta, Y.; Zhu, W. Molecular Engineering of Indoline Based Organic Sensitizers for Highly Efficient Dye-Sensitized Solar Cells. *J. Mater. Chem.* **2012**, *22*, 13348−13356.
(40) Mishra, A.; Fischer, M. K. R.; Bäuerle, P. Metal-Free Organic Dyes for Dye-Sensitized Solar Cells: From Structure: Property Relationships to Design Rules. *Angew. Chem., Int. Ed.* **2009**, *48*, 2474−2499.
(41) Bučar, D.-K.; Henry, R. F.; Lou, X.; Duerst, R. W.; Borchardt, T. B.; MacGillivray, L. R.; Zhang, G. G. Z. Co-Crystals of Caffeine and Hydroxy-2-naphthoic Acids: Unusual Formation of the Carboxylic Acid Dimer in the Presence of a Heterosynthon. *Mol. Pharmaceutics* **2007**, *4*, 339−346.
(42) Gandour, R. D.; Nabulsi, N. A. R.; Fronczek, F. R. A Structural Model of A Short Carboxyl-Imidazole Hydrogen Bond with A Nearly Centrally Located Proton: Implications for the Asp-His Dyad in Serine Proteases. *J. Am. Chem. Soc.* **1990**, *112*, 7816−7817.
(43) Thavasi, V.; Renugopalakrishnan, V.; Jose, R.; Ramakrishna, S. Controlled Electron Injection and Transport at Materials Interfaces in Dye Sensitized Solar Cells. *Mater. Sci. Eng., R* **2009**, *63*, 81−99.
(44) Song, D.; Kang, M.-S.; Lee, Y.-G.; Cho, W.; Lee, J. H.; Son, T.; Lee, K. J.; Nagarajan, S.; Sudhagar, P.; Yum, J.-H. Successful Demonstration of An Efficient $I^-/(SeCN)_2$ Redox Mediator for Dye-Sensitized Solar Cells. *Phys. Chem. Chem. Phys.* **2012**, *14*, 469−472.